Metals and Materials International (2019) 25:1500–1510
https://doi.org/10.1007/s12540-019-00420-1

Effects of the Surface Contact on the Uncertainty in Indentation Yield Strength: Surface Roughness and Angular Misalignment

Oh Min Kwon[1] · Jongho Won[1,2] · Jong-hyoung Kim[1] · Changhyun Cho[1] · Eun-chae Jeon[3] · Dongil Kwon[1]

Received: 2 July 2019 / Accepted: 5 August 2019 / Published online: 16 August 2019

Abstract
We suggest a method for accurately estimating the uncertainty of indentation yield strength determined from the modified Meyer relation as a mathematical function of the measurement, taking into account Type A and Type B uncertainty. Using this method, we quantitatively compared the expanded uncertainty level of the yield strength as measured by instrumented indentation testing (IIT) and uniaxial tensile testing, and propose a dominant measurand that affects the final expanded uncertainty of the indentation yield strength. To interpret the difference in uncertainty between IIT and uniaxial tensile testing, we investigated the effect of the major sources of uncertainty in the IIT system: sample surface roughness and angular misalignment between the surface normal of the sample and the symmetric axis of the indenter. The surface roughness was controlled using 400-, 1000- and 2000-grit paper and the misalignment angle ranged over 0°, 1° and 2°. Acceptable surface roughness and standard uncertainty of misalignment angle are proposed that give the IIT similar uncertainty to uniaxial tensile testing.

Keywords Indentation · Yield strength · Metals · Uncertainty · Spherical indenter

1 Introduction

Instrumented indentation testing (IIT), developed from conventional hardness testing, can evaluate hardness and elastic modulus without optical measurement through elasto plastic analysis of the continuously measured load and depth curves [1, 2]. In addition, it can be used at various scales from micro-scale to nano-scale by controlling the size of the indenter and the load or depth range [3]. Studies have been conducted for decades now on using IIT to evaluate tensile properties [4–6] as well as hardness and elastic modulus. Tensile properties are basic to structural design and are used in reliability assessment to predict material plastic deformation and fracture. Conventional uniaxial tensile testing requires samples of specific shapes [7], and because it is a destructive test method, it is of limited use in assessing the reliability of in-field structures. IIT, on the other hand, is non-destructive and thus can be used for in-field reliability. With these merits, recent research has focused on the evaluation of tensile properties using IIT.

Tabor [8] suggested an experimental relationship between flow stress and strain in uniaxial tension and such spherical indentation parameters as indentation load, contact radius and indenter radius. Following Tabor's approach, extensive work on evaluating tensile properties using the spherical indentation has been conducted. Ahn and Kwon [9] suggested a new definition of flow strain expressed by the shear strain at the contact edge beneath the spherical indenter and investigated the ratio of mean indentation pressure to flow stress in spherical indentation for power-law-hardening metals. Recently, Kang et al. [5], analyzing the stress field beneath a spherical indenter, found that the relation between mean indentation pressure and uniaxial flow stress depends on the material flow properties. In addition, they modified the relationship between yield strength and Brinell hardness (the so-called Meyer relation [10]) and showed good agreement between the

Oh Min Kwon and Jongho Won have equally contributed to this work.

✉ Eun-chae Jeon
jeonec@ulsan.ac.kr

[1] Department of Materials Science and Engineering, Seoul National University, Seoul 08826, Republic of Korea

[2] Centre for Advanced Innovation Technologies (CPIT), VSB-Technical University of Ostrava, 17. listopadu 2172/15, 70800 Ostrava, Czech Republic

[3] School of Materials Science and Engineering, University of Ulsan, Ulsan 44776, Republic of Korea

indentation yield strength and the yield strength measured by uniaxial tensile testing. Although new research on evaluating tensile properties using the IIT continues, little work has been done on uncertainty estimation. Research on the uncertainty in yield strength in particular is needed because the stress variation at the yield point is more severe than at the necking point, increasing the standard uncertainty [7].

According to ISO GUM [11], uncertainty is a parameter expressing doubt about the validity of a measurement result and characterizes the dispersion of a value that could reasonably be attributed to the measurand. Uncertainty is of two classes: Type A and Type B. Type A evaluation is defined as the method involving statistical analysis of experimental data and Type B evaluation is defined as the method based on scientific judgment of all information available on parameter variability except for experimental data. Type A and Type B uncertainty are important for test methods because they are indexes of reliability. Jeon et al. [12] suggested a simplified uncertainty estimation method for indentation tensile properties through measurands defined by a mathematical model. However, they only consider Type A uncertainty, and whether the final expanded uncertainty depends on indentation yield strength was not verified for metallic materials with various hardening behaviors. Moreover, so far the uncertainty difference in the yield strength as measured by the IIT and uniaxial tensile testing remains unclear and it is still unknown how uncertainty sources quantitatively affect the uncertainty of indentation yield strength.

In this study, we use the modified Meyer relation [5] to propose a method for accurately estimating the uncertainty of indentation yield strength by taking into account Type A and Type B uncertainty. A relationship between the uncertainty and the indentation yield strength is demonstrated for metallic materials with various hardening behaviors. Using this method, we quantitatively compared the uncertainty level of the yield strength as evaluated by IIT and uniaxial tensile testing. To determine the dominant measurand affecting the final expanded uncertainty, the degree of contribution (*DOC*) and the coefficient of variation (*CV*) of each measurand were analyzed. Based on these results, we verify the effects of two major uncertainty sources influenced by surface contact: indentation sample surface roughness and angular misalignment between the surface normal of the sample and the symmetric axis of the indenter. The surface roughness was controlled using 400-, 1000- and 2000-grit paper and the misalignment angle ranged over 0°, 1° and 2°. From the relationships between the uncertainty and the major uncertainty sources, acceptable surface roughness and standard uncertainty of the angular misalignment were proposed for which the IIT has uncertainty similar to that of uniaxial tensile testing.

2 Experimental Procedure

Eighteen metallic materials were prepared for instrumented indentation and uniaxial tensile testing: carbon steels S20C, SKD11, SKD61, SKH51, SCM415 and SKS3, aluminum alloys Al2024 and Al7075, copper alloy C10200, titanium alloy Ti–6Al–4V and stainless steels STS303, STS316, STS316L, STS321, STS347, STS410, STS420J2 and STS440C. For IITs, cubic samples of $30\times30\times20$ mm^2 were prepared and one side of the sample was polished with 2000-grit paper according to ISO 14577-1 [13]. A standard hardness block of 200 HV 10 was prepared and one side of it was polished with 400-, 1000- and 2000-grit paper to control surface roughness. Its surfaces were examined by AFM Park NX10 model (Park Systems Inc., Suwon, Korea) with depth resolution 0.015 nm to measure the surface roughness. The maximum vertical and lateral scan length were 100 μm and 100 μm, respectively, and scan rate was 0.25 Hz. IITs were conducted using AIS3000 model (Frontics Inc., Seoul, Korea), with load resolution 0.05 N and depth resolution 0.1 μm; a tungsten carbide spherical indenter of radius 250 μm was used. Indentation depths were every 10 μm from 10 to 150 μm, loading and unloading rates were 0.3 mm/min, multiple unloading down to 50% of maximum load and five repeatable tests were performed for each material. For uniaxial tensile tests, rectangular tensile samples of gauge length 25 mm, thickness 6 mm and width 6 mm were prepared according to ASTM E8/E8M [7]. Five repeatable tests were conducted for each material at crosshead speed 0.5 mm/min on an Instron 5582 (Instron Inc., Grove City, PA, USA).

3 Theoretical Background

3.1 Evaluation of Indentation Yield Strength

Meyer [10] has shown that geometrically similar indentation gives the same Brinell hardness, now called the Meyer relation:

$$\frac{L}{d^2} = C \cdot \left(\frac{d}{D}\right)^{m-2} \tag{1}$$

where L is the indentation load, d is the residual diameter, D is the indenter diameter, C is the material constant and m is the Meyer index determined by fitting. Equation (1) can be rewritten as a relation for the geometrical shape of the spherical indenter as:

$$P_m = \frac{4}{\pi} \cdot C \cdot \left(\frac{a}{R}\right)^{m-2} \tag{2}$$

where P_m is mean indentation pressure, a is contact radius and R is the radius of the spherical indenter. If we consider the constitutive Hollomon equation ($\sigma_t = K \cdot \varepsilon_t^n$, where σ_t,

ε_t, K and n are flow stress, flow strain, strength coefficient and strain-hardening exponent in uniaxial tension) [5], the strain-hardening exponent n is given by

$$n = m - 2 \tag{3}$$

Therefore, Eq. (3) is substituted into Eq. (2) so that the material constant C in Eq. (2) can be rewritten as follows:

$$C = \frac{L}{4 \cdot a^2} \cdot \left(\frac{R}{a}\right)^n = \frac{L \cdot R^n}{4 \cdot a^{n+2}} \tag{4}$$

The contact radius is determined from the contact depth h_c and R from the geometrical contact morphology assuming a perfectly axisymmetric spherical indenter:

$$a = \sqrt{2Rh_c - h_c^2} \tag{5}$$

where h_c is obtained by the Oliver and Pharr [2] equation through a geometrical relationship:

$$h_c = h_{\max} - h_d \tag{6}$$

where $h_{\max}$ is the maximum depth and h_d is the deflection of the surface at the contact perimeter. Here h_d is determined by

$$h_d = \varepsilon \cdot \frac{L_{\max}}{S} \tag{7}$$

where ε is a geometrical constant (0.75 for a spherical indenter) and S is the stiffness determined by the initial slope of the unloading curve.

George et al. [14] found experimentally the following relationship between yield strength and the material constant:

$$\sigma_y = \beta \cdot C \tag{8}$$

where β is a constant depending on the material class; it is reported to be about 0.23 for steel [5].

Kang et al. [5] reanalyzed the Meyer relation [10] using the results of stress-field analysis and the constitutive equation and found that β is related to a combination of strain-hardening exponent, elastic modulus and plastic constraint factor. Using this result, they suggested a modified Meyer relation (Eq. 9) and a quantitative relationship between a modified multiplying constant β' and the strain-hardening exponent (Eq. 10):

$$\sigma_y = \beta' \cdot C^{\frac{1}{1-n}} \tag{9}$$

$$\beta' = f_{\beta'}(p) = -13.43 \cdot n^3 + 11.53 \cdot n^2 - 3.42 \cdot n + 0.36 \tag{10}$$

Because the strain-hardening exponent must be pre-determined in order to predict the yield strength using this modified Meyer relation, Kang et al. [5] proposed a quantitative relationship between the strain-hardening exponent and the ratio of loading slopes:

$$n = f_n(p) = -52.24 \cdot p^3 + 228.18 \cdot p^2 - 329.32 \cdot p + 157.31 \tag{11}$$

where p is the ratio of loading slopes at two fixed contact radii a_1= 150 μm and a_2 = 200 μm in the indentation load and contact radius curve as shown in Fig. 1b:

$$p = \left.\frac{dL}{da}\right|_{a_2} \Big/ \left.\frac{dL}{da}\right|_{a_1} \tag{12}$$

3.2 Evaluation of Uncertainty

We base our uncertainty estimation of the indentation yield strength obtained from the modified Meyer relation on the ISO GUM [11] and the A2LA Guide [15]. The brief procedure for estimating uncertainty has four steps: step 1: set of the mathematical functions for the measurement; step 2: evaluation of the standard Type A and Type B uncertainties; step 3: determination of the combined uncertainties; step 4: determination of the expanded uncertainties. As shown in Fig. 1, measurands in this study are the experimental data directly obtained from the indentation load and depth curves and load and contact radius curves through repeated tests under the same conditions; their values and uncertainties are directly determined in the measurement. The sum of the uncertainties of all measurands affects the uncertainty of the final result. Therefore, to estimate the uncertainty of the indentation yield strength calculated from the modified Meyer relation, we created a

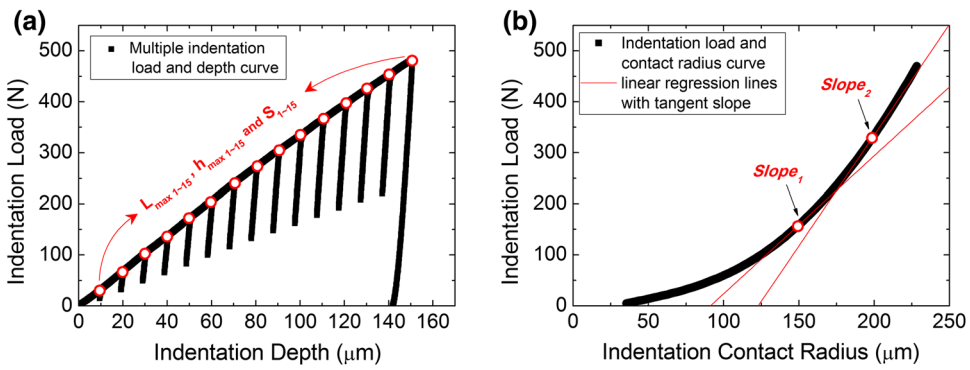

Fig. 1 Measurands determined from **a** multiple indentation load and depth curve **b** indentation load and contact radius curve

mathematical function consisting of the parameters directly obtained from the indentation load and depth curve, not from a mathematical model. Therefore, in order to express Eq. (9) as the measurands (p, S, L and h), the material constant C is rewritten by substituting Eqs. (5–7) into Eq. (4) as follows:

$$C = f(p,S,L,h) = \frac{L\cdot R^{f_n(p)}}{4}\left[(2\cdot R\cdot h)+\left(\frac{3\cdot L\cdot(h-R)}{2\cdot S}\right)-h^2-\left(\frac{9\cdot L^2}{16\cdot S^2}\right)\right]^{-\frac{f_n(p)}{2}-1} \tag{13}$$

where $f_n(p)$ is the cubic function of the ratio of loading slope to determine the strain-hardening exponent (Eq. 11). Finally, Eq. (9) can be expressed as the measurands by substituting Eqs. (10), (11) and (13) into Eq. (9) as follows:

$$\sigma_y = f(p,S,L,h) = f_{\beta'}(p)\left[\frac{L\cdot R^{f_n(p)}}{4}\cdot\left[(2\cdot R\cdot h)+\left(\frac{3\cdot L\cdot(h-R)}{2\cdot S}\right)-h^2-\left(\frac{9\cdot L^2}{16\cdot S^2}\right)\right]^{-\frac{f_n(p)}{2}-1}\right]^{\frac{1}{1-f_n(p)}} \tag{14}$$

where $f_{\beta'}(p)$ is the function of the ratio of loading slope to determine a modified multiplicative constant β' (Eq. 10) given by substituting Eqs. (11) into (10).

The evaluation of uncertainty is classified into Type A and Type B. Type A evaluation is defined as the method by the statistical analysis of experimental data, and Type B evaluation is defined as the method based on scientific judgment using all information available on parameter variability except the experimental data. Since all uncertainties must be converted to standard uncertainties and expressed at the same confidence level, both Type A and Type B uncertainties are expressed as standard uncertainties. Therefore, we estimated the Type A uncertainties of the ratio of loading slope and stiffness through repeated indentation tests and calculated the standard uncertainties $\left(u_{i,A}\right)$ using the following equations:

$$\bar{x} = \frac{1}{j}\sum_{i=1}^{j} x_i \tag{15}$$

$$u_{i,A} = \sqrt{\frac{1}{j}\sum_{i=1}^{j}\left(x_i-\bar{x}\right)^2} \tag{16}$$

where x_i is the repeatedly measured experimental data, $\bar{x}$ is the average value and j is the number of experiments. We then estimated the Type B uncertainties using the resolution of the load and depth sensor and calculated the standard uncertainties $\left(u_{i,B}\right)$ using the rectangle distribution:

$$u_{i,B} = \frac{r}{\sqrt{3}} \tag{17}$$

where r is the resolution of the load and depth sensor.

In order to combine the uncertainties, their units must be the same. So, the standard uncertainties of Type A and Type B are combined by a root-sum-square method and this result is defined as the combined standard uncertainty. The coefficients of sensitivity $\left(c_p, c_S, c_L, c_h\right)$, which are a type of weighting values, were calculated using Eq. (14) as:

$$c_p = \frac{\partial\sigma_y}{\partial p},\quad c_S = \frac{\partial\sigma_y}{\partial S},\quad c_L = \frac{\partial\sigma_y}{\partial L}\quad\text{and}\quad c_h = \frac{\partial\sigma_y}{\partial h} \tag{18}$$

Using Eqs. (15–18), we estimated the combined standard uncertainty $\left(u_c\right)$ as:

$$u_c^2 = \sum_i^N\left(\frac{\partial f}{\partial x_i}\right)^2\cdot u_i^2 = c_p^2\cdot u_p^2 + c_S^2\cdot u_S^2 + c_L^2\cdot u_L^2 + c_h^2\cdot u_h^2 \tag{19}$$

Equation (19) is valid if two or more measurands are independent [11]. The measurands used in Eq. (19) can be considered independent because they are not chemical but physical measurands [12]. To estimate the coverage factor (k), the confidence level of the standard uncertainty must be considered. In general, k is adopted at a 95.45% confidence level and the effective degree of freedom $\left(v_{eff}\right)$ is determined by the Welch–Satterthwaite formula. Thus, the k value was determined using Student's t-table:

$$v_{eff} = \frac{u_c^4(y)}{\sum_{i=1}^{N}\frac{\left[c_i u(x_i)\right]^4}{v_i}} \tag{20}$$

where v_i is the degrees of freedom. Finally, the expanded uncertainty $\left(U_{\sigma_y}\right)$ was estimated using Eq. (21) and expressed as the relative percent value normalized by the indentation yield strength as shown in Eq. (22):

$$U_{\sigma_y} = k\cdot u_c \tag{21}$$

$$U_{\sigma_y}(\%) = \frac{U_{\sigma_y}}{\overline{\sigma_y}}\times 100 \tag{22}$$

The uncertainties were calculated following the flow chart in Fig. 2.

4 Results and Discussion

4.1 Uncertainty of IIT and Uniaxial Tensile Testing

Figure 3 shows five indentation load and depth curves obtained under the same test conditions using the same AIS 3000 equipment for carbon steel SKD11 and copper alloy C10200 among eighteen metallic materials. Their yield strengths as obtained from uniaxial tensile tests are

413.30 MPa and 212.20 MPa, respectively. Using these indentation load and depth curves, the indentation yield strength was determined by the modified Meyer relation (Eq. 9) and the expanded uncertainty of the indentation yield strength was calculated considering Type A and Type B uncertainty in Sect. 3.2. Table 1 shows the standard uncertainties, degree of freedom, k and the expanded uncertainties for the indentation yield strength for the 18 metallic materials. The expanded uncertainties of the indentation yield strength range from 2.12 to 18.69%, with average value 10.46% and standard deviation 5.54%.

As described in Eq. (22), the final expanded uncertainties are the relative percent values influenced by the average values of the yield strength. Therefore, we must demonstrate whether the expanded uncertainty is dependent on the indentation yield strength or not. Figure 4a shows the relationship between the expanded uncertainty and the indentation yield strength. These expanded uncertainties have a negative relationship with the indentation yield strength with polynomial regression line with slope 0.01×10^{-1}, and the p value is evaluated at 0.93. We see from this result that there is no correlation between the expanded uncertainty expressed as relative value and the indentation yield strength because the

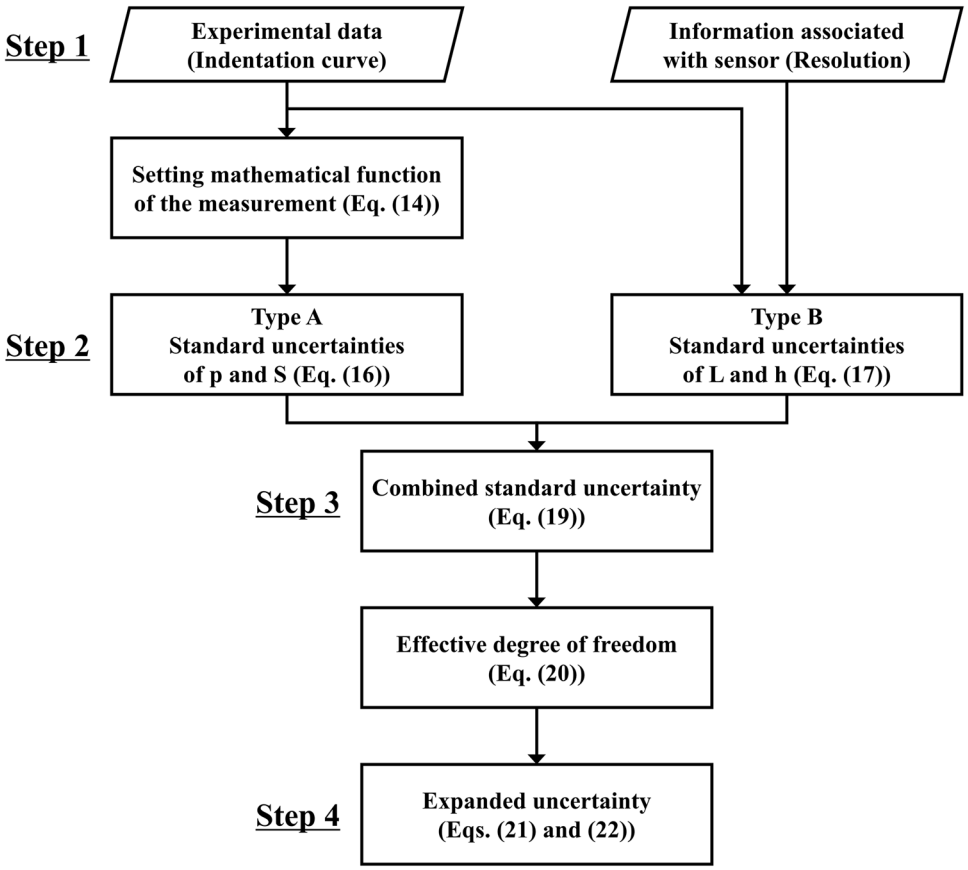

Fig. 2 Schematic flow chart for estimating uncertainty of indentation yield strength

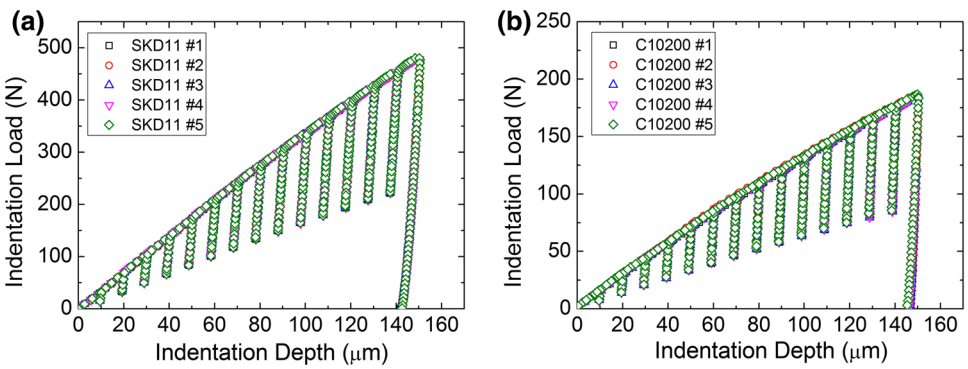

Fig. 3 Five indentation load and depth curves for **a** SKD11 and **b** C10200 from AIS 3000 model

Table 1 Uncertainty table for the indentation yield strength

Materials	Standard uncertainties				v_{eff}	k	U_{σ_y} (%)
	p	S (N/μm)	L (N)	h (μm)			
SCM415	0.010	1.623	0.032	0.058	4.000	2.870	17.889
SKD11	0.002	0.806			4.001		2.662
SKD61	0.003	4.504			4.004		5.442
SKH51	0.004	3.982			4.003		6.029
SKS3	0.001	1.349			4.004		2.124
S20C	0.006	10.723			4.002		10.615
Al2024	0.012	1.395			4.000		18.694
Al7075	0.002	1.048			4.005		2.905
C10200	0.006	0.529			4.000		9.796
Ti–6Al–4V	0.010	0.753			4.000		15.949
STS303	0.012	7.857			4.000		16.746
STS316	0.006	5.256			4.000		9.719
STS316L	0.013	4.671			4.000		17.631
STS321	0.005	3.259			4.001		6.775
STS347	0.012	3.932			4.000		17.136
STS410	0.004	1.987			4.000		6.326
STS420J2	0.007	6.583			4.001		11.091
STS440C	0.007	7.085			4.003		10.817

p value is much greater than 0.05 with a 95% confidence level [16]. Therefore, the expanded uncertainties estimated in this study are influenced not by yield strength but by uncertainty sources.

The uncertainty of the uniaxial tensile testing was estimated using the example in A2LA [15]. The mathematical function of yield strength is:

$$\sigma_y = f(L, T, W) = \frac{L}{T \cdot W} \tag{23}$$

where L is the load at the 0.2 offset yield point in the stress and strain curve, T is the thickness and W is the width of the rectangular tensile sample. The uncertainty of the yield strength was calculated based on Sect. 3.2. Table 2 presents the standard uncertainties, degree of freedom, k and the expanded uncertainties for the yield strength obtained from the uniaxial tensile test. The expanded uncertainties of the yield strength range from 0.92 to 12.60%, with average value 5.08% and standard deviation 3.36%. The expanded uncertainties of the indentation yield strength present a larger and wider dispersion than that of the uniaxial tensile testing. This means that the IIT system can be affected by uncertainty sources different from the uniaxial tensile testing, as discussed in Sect. 4.3.

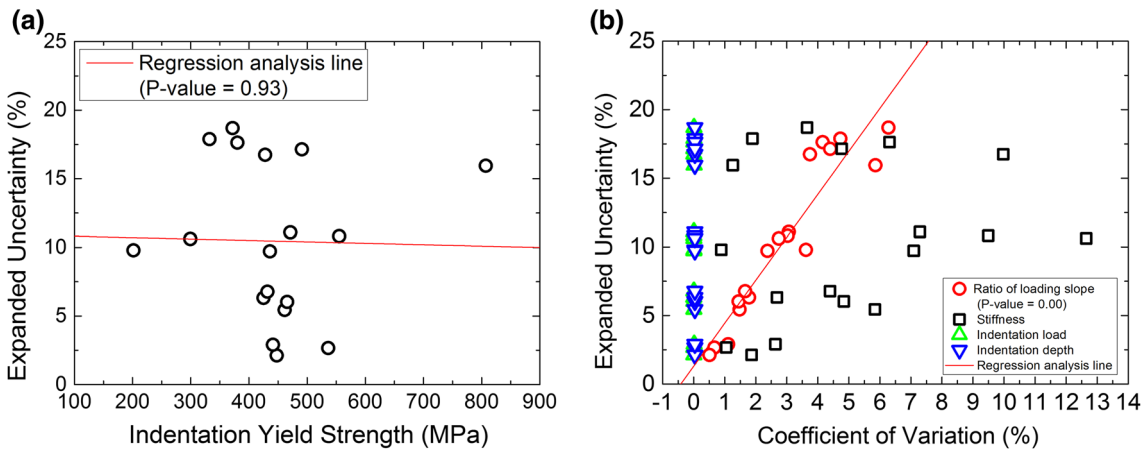

Fig. 4 Regression analysis of expanded uncertainty with **a** indentation yield strength **b** coefficient of variation for measurands

Table 2 Uncertainty table for the yield strength obtained from uniaxial tensile testing

Materials	Standard uncertainties			v_{eff}	k	U_{σ_y} (%)
	L (N)	T (mm)	W (mm)			
SCM415	396.077	0.013	0.007	4.030	2.870	11.875
SKD11	176.440	0.021	0.012	4.717	2.650	3.741
SKD61	45.074	0.013	0.007	8.831	2.320	0.917
SKH51	104.320	0.013	0.015	5.409	2.650	2.286
SKS3	254.519	0.010	0.006	4.117	2.870	4.792
S20C	279.669	0.010	0.008	4.044	2.870	8.381
Al2024	161.294	0.008	0.010	4.309	2.870	3.227
Al7075	118.956	0.006	0.014	5.277	2.520	1.698
C10200	334.388	0.008	0.010	4.019	2.870	12.597
Ti–6Al–4V	240.841	0.010	0.014	5.024	2.520	2.133
STS303	138.414	0.013	0.010	4.324	2.870	4.066
STS316	71.605	0.005	0.010	4.506	2.650	1.990
STS316L	91.488	0.006	0.005	4.129	2.870	3.040
STS321	250.887	0.013	0.007	4.120	2.870	5.959
STS347	144.589	0.007	0.006	4.281	2.870	2.859
STS410	434.319	0.007	0.010	4.039	2.870	8.169
STS420J2	240.711	0.015	0.004	4.136	2.870	5.641
STS440C	285.062	0.010	0.005	4.036	2.870	8.139

4.2 Effects of Measurands on Uncertainty of Indentation Yield Strength

The measurands obtained directly from the experiment affect the final uncertainty of the mathematical function. So, if the dominant measurand can be determined, the uncertainty of the mathematical function can be controlled. The degree of contribution (*DOC*) [17] was calculated to analyze quantitatively the contribution of the measurands to the expanded uncertainty. The *DOC* of measurands is defined as:

$$DOC(\%) = \frac{c_i^2 u_i^2}{u_c^2} \times 100 \tag{24}$$

The *DOCs* of the measurands to the expanded uncertainty are shown in Table 3. The *DOCs* of the ratio of loading slope are about 99% for all eighteen metallic materials, the largest among the measurands. On the other hand, the *DOCs* of stiffness, load and depth are all less than 1%. Therefore, the expanded uncertainty of indentation yield strength is dominated by the ratio of loading slope.

In addition to *DOC*, we introduce a coefficient of variation (*CV*) [17] as another statistic to confirm that the expanded uncertainty of indentation yield strength is dominated by the variation in the ratio of loading slope. The *CV* is a value that can be used to compare distributions of groups when the difference in the average values of groups is very large due to different units. The *CV* of the population is defined as:

Table 3 Degree of contribution of measurands on expanded uncertainty of indentation yield strength

Materials	p (%)	S (%)	$L_{\max}$ (%)	$h_{\max}$ (%)
SCM415	99.996	0.002	0.000	0.002
SKD11	99.795	0.104	0.004	0.096
SKD61	99.491	0.486	0.001	0.022
SKH51	99.679	0.302	0.001	0.018
SKS3	99.417	0.427	0.009	0.147
S20C	99.760	0.233	0.001	0.006
Al2024	99.971	0.027	0.000	0.002
Al7075	99.203	0.720	0.008	0.069
C10200	99.991	0.001	0.003	0.005
Ti–6Al–4V	99.989	0.008	0.000	0.002
STS303	99.873	0.125	0.000	0.002
STS316	99.740	0.252	0.000	0.007
STS316L	99.965	0.034	0.000	0.001
STS321	99.843	0.146	0.001	0.011
STS347	99.973	0.026	0.000	0.002
STS410	99.914	0.068	0.001	0.016
STS420J2	99.873	0.122	0.000	0.005
STS440C	99.545	0.450	0.000	0.005

$$CV(\%) = \frac{u_i}{\bar{x}} \times 100 \tag{25}$$

Figure 4b presents the relationship between *CV* of measurands and the expanded uncertainty. The *CVs* of the ratio of loading slope and the expanded uncertainties are positively

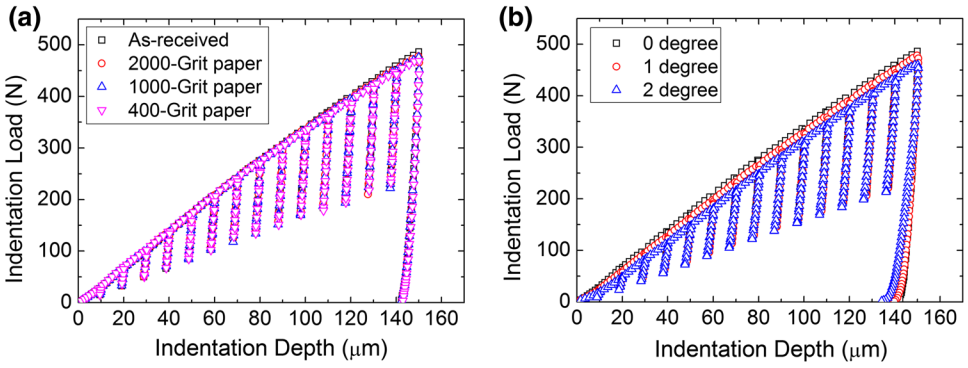

Fig. 5 Effect of **a** surface roughness and **b** angular misalignment on indentation load and depth curve for standard block with 200 HV 10

correlated with the polynomial regression line with slope 3.13, and the p value is evaluated at 0.01×10^{-6}. The *CVs* of the stiffness and the expanded uncertainties are positively correlated with polynomial regression line with slope 0.38, but these data points are scattered around the polynomial regression line. The *CVs* of the indentation load and the *CVs* of the indentation depth were about 0.01 and 0.04, respectively. They were almost the same for all materials because the indentation load and depth were evaluated as Type B uncertainty. Thus, the *CV* of the ratio of loading slope is more strongly correlated with the expanded uncertainty than the *CVs* of other measurands. This means that the standard uncertainty and the expanded uncertainty of the indentation yield strength are dominated by the variation in the ratio of loading slope, as with the *DOC* results. This result can be qualitatively understood from the uncertainty function (Eq. 14), which contains an exponential term of the ratio of loading slope. Thus, if the uncertainty sources causing the slope variation in the indentation loading curve are controlled, the uncertainty of indentation yield strength can be significantly reduced.

4.3 Effects of Uncertainty Sources on Uncertainty of Indentation Yield Strength

As shown in Tables 1 and 2, the expanded uncertainties of indentation yield strength show larger and wider dispersion than that of uniaxial tensile testing. Diverse sources affect the uncertainty more or less seriously: test system (test sample, experimental equipment, etc.), environment, operator, etc. [18]. We focused on the material-extrinsic uncertainty sources that can occur in the test system, not material-intrinsic uncertainty sources (e.g. grain-size heterogeneity). In addition, we assumed the uncertainty sources other than those of the test system are negligible because a single operator performed the IITs and the uniaxial tensile tests in the same laboratory. For the test system, as the IIT evaluates local properties by mechanical contact between indenter and material surface, uncertainty sources influenced by the surface contact mainly affect the final uncertainty of the IIT, unlike in uniaxial tensile testing. One of the uncertainty sources influenced by the surface contact is sample surface roughness [19, 20]. This surface roughness cannot be completely eliminated, since no surface is perfectly flat, and this affects the indentation load and depth curve. If the indenter is located on a peak, the material is deformed to a greater indentation depth at relatively low load; if it is located in a valley, the opposite is observed on a rough-surface sample at nano-scale. Thus, the indentation load and depth curves are scattered depending on whether indentation is conducted on a peak or in a valley [21]. Although surface roughness in micro-indentation is less influential than during nano-indentation, it remains nevertheless one of the sources affecting uncertainty of the IIT. In general, it is difficult to control acceptable surface roughness in the field, so the uncertainty level influenced by surface roughness must be verified.

A standard hardness block with 200 HV 10 was chosen as the reference material to verify the effect of surface roughness. We controlled the surface roughness using 400-, 1000- and 2000-grit paper on the as-received hardness block, which was manufactured through polishing and wet buffing. IITs were performed for the four types of surface roughness, the indentation load and depth curves for which are presented in Fig. 5a. The indentation yield strength and expanded uncertainty were then calculated based on Sect. 3. Figure 6a shows the effect of the expanded uncertainty depending on the surface roughness R_a for the standard-hardness block with 200 HV 10 and nine metallic materials. The expanded uncertainty and R_a are positively correlated with the polynomial regression line with slope 0.24, and the p value is evaluated at 0.03×10^{-3}. For the hardness block polished with 400-grit paper, the expanded uncertainty is about 17.71%, almost double that of the hardness block polished with 1000-grit paper. For the hardness block polished with 1000-grit paper, the expanded uncertainty is about 10.49%, similar to the hardness block polished with 2000-grit paper. For the hardness block polished with 2000-grit paper, R_a is about 13.53 nm and the expanded uncertainty is about 8.38%, a significant 6.26-fold increase

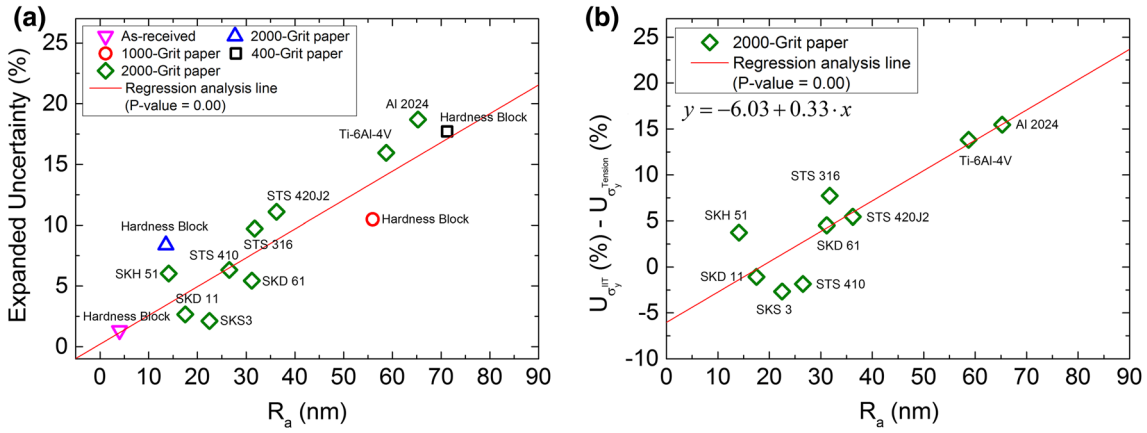

Fig. 6 Effects of surface roughness on **a** expanded uncertainty of indentation yield strength and **b** difference between expanded uncertainty of IIT and uniaxial tensile testing for standard block with 200 HV 10 and metallic materials

over the as-received hardness block (for which R_a is about 4.01 nm and the expanded uncertainty is about 1.34%). This result can be simply explained. The change in the standard uncertainty of the ratio of loading slope depending on R_a. R_a of about 13.53 nm, 55.95 nm and 71.25 nm leads to a slight 0.99-, 0.97- and 0.98-fold decrease, respectively, in the average of the ratio of loading slope, but leads to a significant 6.29-, 7.67- and 12.58-fold increase, respectively, in the standard uncertainty of the ratio of loading slope compared to R_a 4.01 nm. Thus, this significantly increased standard uncertainty of the ratio of loading slope increases the final expanded uncertainty of the indentation yield strength.

The metallic materials in Fig. 6a were selected for each of three materials in ranges of uncertainty differences between the IIT and the uniaxial tensile tests of less than about 3%, from about 3 to about 5%, and more than about 7%, as shown in Table 1. These metallic materials polished with 2000-grit paper have difference values of R_a and their expanded uncertainty increases linearly depending on increasing R_a, as in the results of the hardness block. From this result, we analyzed the trend of expanded uncertainty differences between IIT and uniaxial tensile testing ($U_{\sigma_y^{IIT}}(\%) - U_{\sigma_y^{Tension}}(\%)$) depending on R_a to confirm whether surface roughness is an uncertainty source that makes the uncertainty of IIT larger than that of uniaxial tensile testing. The metallic materials with larger expanded uncertainty of IIT than that of uniaxial tensile testing are presented in Fig. 6b; we see that the expanded uncertainty differences between IIT and uniaxial tensile testing are proportional to R_a, and the p value is evaluated at 0.02×10^{-1}. Therefore, surface roughness is one of the uncertainty sources that make the uncertainty of IIT larger than that of uniaxial tensile testing. Considering the same uncertainty of IIT and uniaxial tensile testing, we recommend an R_a of about 18 nm or less for indentation samples, as determined by the linear regression analysis function ($y = -6.03 + 0.33 \cdot x$) obtained from the relationship between the expanded uncertainty difference and R_a.

In addition to the effect of surface roughness, another issue affecting the uncertainty of the IIT is the angular misalignment between the surface normal of the sample and the symmetric axis of the indenter [20]. Due to the structural tolerance of the experimental equipment and the sample imperfection caused by mechanical polishing, the sample surface cannot be perfectly perpendicular to the indenter. Angular misalignment causes incomplete contact between the indenter and material surfaces that degrades the accuracy and reproducibility of the indentation load and depth curves [22]. Thus, we explored the effect of angular misalignment on the uncertainty of indentation yield strength. To control the angular misalignment between the surface normal of the sample and the symmetric axis of the indenter, the angle of the sample was adjusted with the indenter's angle fixed. The IITs were performed four times per misalignment angle over 0°, 1° and 2° for an as-received standard hardness block with 200 HV 10, the indentation load and depth curves for which are presented in Fig. 5b. The indentation yield strength and the expanded uncertainty were then estimated for combinations of four indentation load and depth curves with the same standard uncertainty of misalignment angles. The effect of angular misalignment on expanded uncertainty of indentation yield strength is shown in Fig. 7. When the four IITs with the same angle 0° were carried out, the expanded uncertainty was about 1.34%. For the range from about 0.4° to 0.5° of standard uncertainty of misalignment angle, the maximum expanded uncertainty is 8.42%. For the range from about 0.7° to 1.0° of standard uncertainty of misalignment angle, the maximum expanded uncertainty is 27.81%. This result can be clarified by the change in the

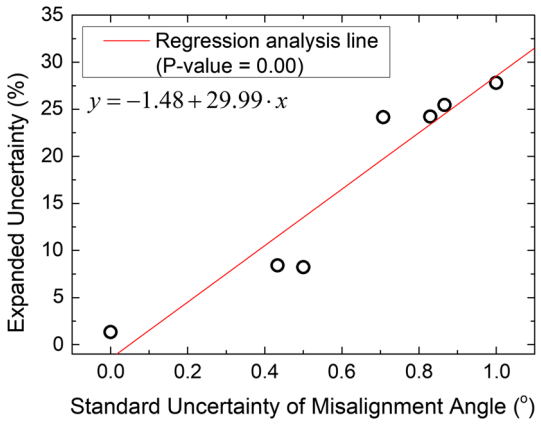

Fig. 7 Effect of angular misalignment on expanded uncertainty of indentation yield strength for standard block with 200 HV 10

ratio of loading slope depending on angular misalignment. Misalignment angles of 1° and 2° lead to a slight 1.02- and 1.09-fold increase, respectively, in the average of the ratio of loading slope, but lead to a significant 7.24- and 13.02-fold increase, respectively, in the standard uncertainty of the ratio of loading slope compared to 0°. Therefore, if the surface of the sample is not perfectly perpendicular to the indenter, irregular ratios of loading slope will be evaluated in each IIT, which increases the uncertainty of indentation yield strength determined from combination of irregular loading slope ratios. From the linear regression analysis function ($y = -1.48 + 29.99 \cdot x$) obtained from the relationship between the expanded uncertainty and the standard uncertainty of misalignment angle, when the standard uncertainty of the misalignment angle is under about 0.22°, it is expected that the expanded uncertainty of IIT is similar to an average expanded uncertainty of 5.08% in the uniaxial tensile testing statistically analyzed here.

5 Conclusions

We propose a method for accurately estimating the uncertainty of indentation yield strength determined from the modified Meyer relation as a mathematical function of the measurement, taking into account Type A and Type B uncertainty based on the ISO GUM and the A2LA guide. The expanded uncertainties of the indentation yield strength for the 18 metallic materials studied range from 2.12 to 18.69%, with average value 10.46% and standard deviation 5.54%, which is wider and larger than that of the uniaxial tensile testing. The expanded uncertainties estimated here are influenced not by the indentation yield strength but by uncertainty sources because the p value at 95% confidence level is much greater than 0.05. The *DOCs* of the ratio of loading slope is about 99% for all 18 metallic materials, and the *CVs* of the ratio of loading slope are most strongly correlated with the expanded uncertainties among measurands. Thus, we concluded that the expanded uncertainty of indentation yield strength is dominated by the ratio of loading slope. The expanded uncertainty of the indentation yield strength increases with increasing surface roughness parameter, R_a and increasing standard uncertainty of misalignment angle. It is recommended that the acceptable surface roughness and standard uncertainty of misalignment angle must be below about 18 nm and 0.22°, respectively, for the IIT to have uncertainty similar to uniaxial tensile testing.

Acknowledgements This research was supported by Basic Science Research Program through the National Research Foundation of Korea (NRF) funded by the Ministry of Education (2019R1I1A3A01054545) and the Ministry of Science and ICT (No. NRF-2015R1A5A1037627).

References

1. M.F. Doerner, W.D. Nix, J. Mater. Res. **1**, 601 (1986)
2. W.C. Oliver, G.M. Pharr, J. Mater. Res. **7**, 1564 (1992)
3. A. Kruk, A.M. Wusatowska-Sarnek, M. Ziętara, K. Jemielniak, Z. Siemiątkowski, A. Czyrska-Filemonowicz, Met. Mater. Int. **24**, 1036 (2018)
4. S.H. Kim, M.K. Baik, D. Kwon, J. Eng. Mater. Technol. **127**, 265 (2005)
5. S.K. Kang, Y.C. Kim, K.H. Kim, J.Y. Kim, D. Kwon, Int. J. Plast. **49**, 1 (2013)
6. T.H. Pham, S.E. Kim, J. Mater. Sci. Eng. A. **688**, 352 (2017)
7. ASTM E8/E8M-16a, *Standard Test Method for Tension Testing of Metallic Materials* (American Standard for Testing of Materials, Philadelphia, 2016)
8. D. Tabor, *The Hardness of Metals* (Clarendon Press, Oxford, 1951), pp. 19–94
9. J.H. Ahn, D. Kwon, J. Mater. Res. **16**, 3170 (2001)
10. E. Meyer, Phys. Z. **9**, 66 (1908)
11. ISO/IEC GUIDE 98-3, *Uncertainty of Measurement-Part 3: Guide to the Expression of Uncertainty in Measurement* (International Organization for Standardization, Geneva, 2008)
12. E.C. Jeon, J.S. Park, D.S. Choi, K.H. Kim, D. Kwon, J. Eng. Mater. Technol. **131**, 6 (2009)
13. ISO/FDIS 14577-1, *Metallic Materials-Instrumented Indentation Test for Hardness and Materials Parameters—Part 1: Test method* (International Organization for Standardization, Geneva, 2002)
14. R.A. George, S. Dinda, A.S. Kasper, Met. Prog. **109**, 30 (1976)
15. T.M. Adams, A2LA Guide for the estimation of measurement uncertainty in testing, Chap. 3 (The American Association for Laboratory Accreditation, Frederick, 2002)
16. C.J. Chieh, Linear regression: making sense of a six sigma tool (2008). https://www.isixsigma.com/tools-templates/regression/linear-regression-making-sense-six-sigma-tool/. Accessed 8 Jan 2019
17. R. Kessel, R. Kacker, M. Berglund, Metrologia **43**, S189 (2006)

18. S. Adamczak, J. Bochnia, B. Kaczmarska, Metrol. Maeas. Syst. **21**, 553 (2014)
19. ASTM E2546-15, *Standard Practice for Instrumented Indentation Testing* (American Society for Testing and Materials, West Conshohocken, 2015)
20. G.E. Dieter, *Mechanical Metallurgy* (McGraw-Hill Book Company, London, 1988), pp. 332–334
21. Y. Xia, Ph.D. Thesis, Université de Technologie de Compiègne, 2014
22. N.B. Shahjahan, Z. Hu, J. Mater. Res. **32**, 1456 (2017)